Energy Storage Materials 24 (2020) 689–693

Contents lists available at ScienceDirect

Energy Storage Materials

journal homepage: www.elsevier.com/locate/ensm

Rolling press of lithium with carbon for high-performance anodes

Na Shu [a,1], Jian Xie [a,1], Xinyuan Wang [a,1], Xiaodong He [a], Lina Xiao [a], Fei Pan [a], Hong Yuan [a], Jianglin Ye [a], Chunhua Chen [a], Yanwu Zhu [a,b,*]

[a] CAS Key Laboratory of Materials for Energy Conversion & Department of Materials Science and Engineering, University of Science and Technology of China, Hefei, Anhui, 230026, PR China

[b] Hefei National Research Center for Physical Science at the Microscale, IChEM (Collaborative Innovation Center of Chemistry for Energy Materials), University of Science and Technology of China, Hefei, Anhui, 230026, PR China

ARTICLE INFO

Keywords:
Carbon
Lithium metal anode
Rolling press

ABSTRACT

Many lithium (Li) metal anodes reported so far have been prepared by electrodeposition of Li on current collectors, for which sacrificing cells are needed in the practical applications. In this work, Li foils are compressed with various carbons such as reduced graphite oxide (rGO), activated microwave exfoliated GO (aMEGO) and activated carbon (AC) by rolling press, resulting in C/Li composites for Li metal anodes. The electrochemical evaluations show that all the three composite anodes are cyclable for 1500 h at a current density of 10 mA cm^{-2} for a capacity of 10 mA h cm^{-2}. Specifically, the rGO/Li anode shows relatively lower overpotentials and more stable cycling performance than the other two. Characterizations indicate that the high pore volume and the moderate pore size of the rGO powder benefit the Li migration and the tolerance to volume change during Li plating/stripping, demonstrating a more stable electrode-electrolyte interface in the cycling. The study provides a potentially scalable and cost-effective strategy for the production of high-performance Li metal anodes.

1. Introduction

Conventional graphite anodes for lithium (Li) ion batteries cannot meet the future high energy-density demand due to the limited theoretical capacity. Alternatively, the Li metal is considered as an ideal candidate for anodes owing to the large theoretical capacity (3860 mA h g^{-1}), low redox potential (−3.04 V vs standard hydrogen electrode) and low density (0.534 g cm^{-3}) [1]. However, the nearly infinite relative dimensional change and unstable solid electrolyte interphase (SEI) result in the formation of Li dendrites and the deterioration of Coulombic efficiency (CE) with cycling, which may cause significant issues related to safety and cycling life when the bare Li metal is directly used as anodes [2]. To solve above problems, strategies have been recently developed via 1) pre-forming stable SEI films [3–7] or 'repairing' the unstable SEI films by adding stabilization agents into electrolytes [8,9], and 2) accommodating metallic Li into proper hosts to prevent the random yet continuous growth of Li dendrites and meanwhile to alleviate the volume change [10–16]. In the proceedings mentioned above, many Li metal anodes reported so far have been prepared by the electrodeposition of Li ions on current collectors, for which sacrificing cells are needed for the preparation of Li composites, complicating the use of Li metals in practical applications [4]. Finding methods to pre-store high-fraction Li is essential to develop practical Li metal anodes compatible to production procedures.

One method has focused on the thermal infusion of molten Li. It has been reported that, infusing molten Li into "lithiophilic" hosts, such as reduced graphene oxide (rGO) [10], ZnO-coated polyimide [17], silicon-coated carbon fiber networks [18] and Ag-coated carbon fibers [19], would induce uniform Li deposition, leading to the low overpotentials and small volume changes. For most of materials, however, their relatively weak binding with Li leads to poor lithiophilicity, excluding them as candidates for hosting Li [10]; the surface modulation has also complicated the preparation. In another strategy a spray-painting has been utilized to coat materials such as rGO on Li as an artificial SEI [5], but the preparation of the homogeneous painting suspension involved the solvent processing based on volatile N-methyl--pyrrolidone [5] or tetrahydrofuran [4].

Apart from above techniques, a rolling press has been recently

* Corresponding author. CAS Key Laboratory of Materials for Energy Conversion & Department of Materials Science and Engineering, University of Science and Technology of China, Hefei, Anhui, 230026, PR China.
E-mail address: zhuyanwu@ustc.edu.cn (Y. Zhu).

[1] These authors contributed equally to this work.

https://doi.org/10.1016/j.ensm.2019.07.044
Received 14 May 2019; Received in revised form 13 July 2019; Accepted 29 July 2019
Available online 1 August 2019

reported as a simple mechanical method to fabricate Li composites [20–22]. For example, Yang et al. compressed various layered materials such as Ti_3C_2 MXene, graphene and BN with Li foils, among which Ti_3C_2 MXene demonstrated the ability to restrict the growth of Li dendrites along the nanoscaled gaps between layers, thus preventing their vertical growth to pierce the separators [20]. In observation of the high density of MXene, lighter carbon materials provide low density yet excellent mechanical strength under the redox environment in Li metal batteries [10,23]. Cho et al. investigated the effect of doping on the performance by rolling press of Li with various graphene materials such as rGO, phosphate-functionalized rGO (PrGO) and nitrogen-doped rGO (NrGO), reaching a conclusion that the performance of PrGO is better than NrGO or rGO, as PrGO may stabilize the Li migration by the favored interaction between Li and pyro-/metaphosphates and phosphorus species [21]. Other factors like pore size and surface area of the host affect the performance of Li composite anodes as well [11,24]. For instance, Guo et al. found that three-dimensional (3D) Cu foam with a pore diameter of 170 μm did not suppress Li dendrites, while that with a pore diameter of 2.1 μm could effectively accommodate Li deposition without demonstrating uncontrollable growth of Li dendrites [25]. Hence, to use carbons as media to host Li in rolling press, optimized morphology and microstructure of the carbons are desired to achieve high-performance Li-metal anodes.

Herein, we prepare the carbon/Li composites by using different carbons such as rGO, activated microwave exfoliated GO (aMEGO) and activated carbon (AC) in rolling press (resulting in samples noted rGO/Li, aMEGO/Li, AC/Li, respectively), to investigate the effect of carbon structure on the performance of the composite anodes. It is found that all the three composite anodes are cyclable for 1500 h for a high capacity of 10 mAh cm^{-2}. Among them, the rGO/Li anode shows relatively lower overpotentials and more stable cycling than the other two. Characterizations indicate that rGO are able to effectively accommodate Li during plating but the pores in aMEGO or AC which range between 1 and 4 nm may be too small to host Li and thus a large fraction of Li deposits on the surface of these two carbons rather than into the pores.

2. Experimental section

2.1. Preparation of carbon (rGO, aMEGO, AC)/Li electrodes

Commercial rGO, aMEGO (both purchased from The Sixth Element (Changzhou) Materials Technology Co., Ltd., China) or AC (purchased from Sinopharm Chemical Reagent Co., Ltd., China), and Li circular plates (thickness: 460 μm, diameter: 16 mm, purchased from Wuhan Newthree Technology CO., Ltd., China) were used to prepare the carbon/Li composites. The rolling aperture of the roller (Jingyineng Lithium Electric Equipment Co., Ltd., China) can be tuned from 10 μm to 2 cm. The rolling preparation was performed in an argon-filled glove box with O_2 content less than 0.1 PPM and H_2O content less than 0.1 PPM.

The preparation of carbon (rGO, aMEGO, AC)/Li composites is briefly illustrated in Fig. 1a. Li plates were firstly weighed and recorded exactly. Then, ~1.5 mg of carbon powder was manually distributed on the surface of a fresh Li plate, and the carbon coated plate was gently hand-pressed for binding the carbon with Li, resulting in sample called 1Li+1C. The same amount of carbon powder was placed on the fresh Li surface (without carbon) of 1Li+1C and the plate was gently hand-pressed again, forming a sample 1Li+2C. After that, another 1Li+1C sample was gently hand-pressed for binding with 1Li+2C by facing the fresh Li side of 1Li+1C to 1Li+2C. By repeating the process, a stacking of nLi+(n+1)C was obtained. Finally, the nLi+(n+1)C stacking was roll-pressed to the thickness desired. The carbon content of carbon (rGO, aMEGO, AC)/Li composites was determined by subtracting the mass of Li from the mass of total electrodes. The electrodes were punched into cycloidal electrodes, all with a diameter of 10 mm and then assembled in CR2032 coin cells.

2.2. Characterizations

The morphology of samples was characterized by scanning electron microscopy (SEM, Hitachi, SU8200, Japan). The composition of samples was evaluated by Fourier transform infrared spectroscopy (FTIR, Thermo Nicolet, NICOLET 8700, America),X-ray Diffraction (XRD, Rigaku, D/max-TTR III, Japan) and the X-ray photoelectron spectroscopy (XPS, Thermo-VG Scientific, ESCALAB 250, USA). N_2 adsorption/desorption isotherms were measured with a Quantachrome Autosorb-IQ apparatus (USA).

2.3. Electrochemical measurements

CR2032 coin cells were assembled in an argon-filled glove box using the carbon (rGO, aMEGO, AC)/Li composites with 460 μm thickness as the working electrodes, as-purchased Li foils (Wuhan Newthree Technology CO., Ltd., China) with 460 μm thickness as the counter/reference electrodes to evaluate the cycling stability. Symmetrical CR2032 coin cells were separately assembled with the carbon (rGO, aMEGO, AC)/Li with 100 μm thickness to evaluate the cycling stability. 1 M lithium bis(trifluoromethanesulfonyl)imide in 1,3-dioxolane (DOL)/1,2-dimethoxyethane (DME) (1:1 w/w) with 2 wt% lithium nitrate was used as electrolyte. For the long-time cycling test, the batteries were plated/stripped at 10 mA cm^{-2} for 1 h.

3. Results and discussion

Taking rGO/Li (5Li+6rGO) as an example, after carbon coating and

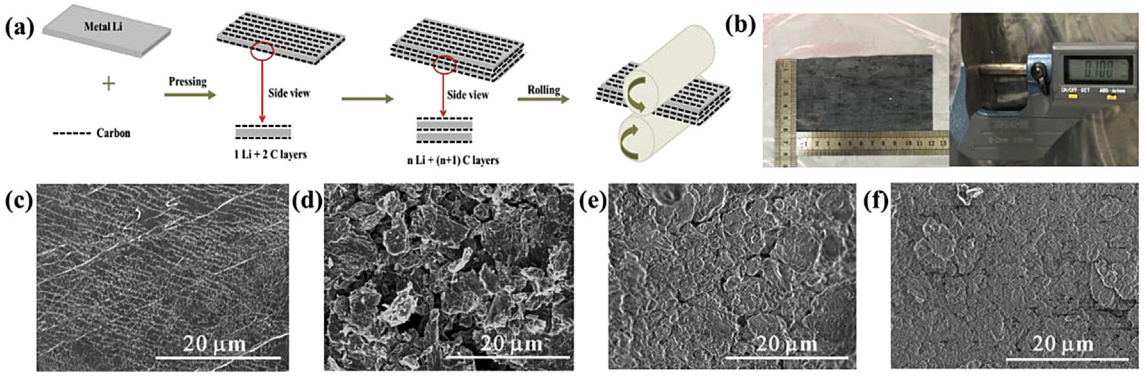

Fig. 1. (a) Schematic of the synthesis of carbon (rGO, aMEGO, AC)/Li composite anodes. (b) Optical image of rGO/Li with size of 6 cm × 12 cm and thickness of 100 μm. White dots are due to the oxidization of Li exposed to ambience. Top view SEM images of (c) Li, (d) rGO/Li (5Li+6rGO), (e) aMEGO/Li (5Li+6aMEGO), and (f) AC/Li (5Li+6AC).

rolling press the originally shiny Li plate was uniformly covered with a layer of dark rGO powder, as shown in the optical image in Fig. 1b. The top view SEM image of Li (Fig. 1c) shows that the surface is nonuniform with steps, while Fig. 1d reveals that carbon flakes are dispersed on the surface of rGO/Li, and Fig. 1c and d reveal that the surface of Li is coated with a more compact carbon layer for aMEGO/Li and AC/Li. The cross-sectional SEM images (Fig. S1, Supporting Information) disclose the multi-layered distribution of the carbon in the composite foil. The energy dispersive spectroscopy (EDS) image, taken in the SEM, shows the homogenous dispersion of C on the surface (Figs. S2, S3, and S4, Supporting Information). On the other hand, oxygen was detected from EDS, which could be introduced from the oxidization of Li and/or the carbon resources, as Fourier transform infrared spectroscopy (FTIR) spectra (Fig. S5, Supporting Information) show that rGO, aMEGO and AC contain O–H (3400–3600 cm^{-1}) and C–O (1000–1260 cm^{-1}) groups [10]. X-ray photoelectron spectroscopy (XPS, Fig. S6 in Supporting Information) shows that the atomic content of O in aMEGO, rGO and AC is 1.83%, 7.08% and 16.05%, respectively. Previous reports mentioned that the O content in carbon is beneficial to inducing uniform Li deposition [10,20]. The X-ray diffraction (XRD) patterns (Fig. S7, Supporting Information) indicate the carbon is mostly amorphous and the Li maintains its structure in the composite.

In order to understand the dependence of carbon content in the composites on the layer number n in the nLi+(n+1)C stacking, rGO/Li composites with the same thickness of 100 μm but from different initial Li layer numbers have been fabricated. As shown in Fig. 2a, the carbon content gradually decreases from more than 11%–~7% as the layer number increases till 8. It is worth noting that the rolling press to 100 μm would be challenging for more Li layers due to the rolling hardening of Li foils. In order to elaborate the effect of n in nLi+(n+1)C in terms of Li migration, symmetrical cells were assembled using 3Li+4rGO, 4Li+5rGO, 5Li+6rGO, or 6Li+7rGO all with 100 μm thickness as the electrode, respectively, and the electrochemical impedance spectroscopy (EIS) was carried out. As shown in Fig. 2b and Table S1 (Supporting Information), the interface resistance decreases as the layer number increases, indicating the faster kinetics of Li migration and the better interface in the composites [26]. Because of higher degree of Li rolling pressure for the more Li layers but with the same final thickness, the carbon would be dispersed more uniformly in the composites. Thus, the Li/C interface could be more stable in the composites from more initial Li layers, leading to the lower energy barrier for Li migration. In the following, 5Li+6C and 10Li+11C were chosen for the systematical studies. But due to the rolling hardening mentioned above, 10Li+11C was prepared for the final thickness of 460 μm. The density of 5Li+6C and 10Li+11C has listed in Table S2 (Supporting Information).

To evaluate the cycling performance of the carbon/Li composite anodes, the voltage variation was monitored during the Li plating/stripping in half cells made of the composite anodes. Fig. 3a shows the voltage profiles of rGO/Li, aMEGO/Li and AC/Li anodes with the thickness of 460 μm. When a high current of 10 mA cm^{-2} is used for a cycling capacity of 10 mA h cm^{-2} (corresponding to a Li utilization of ~11.2%, 13.2% or 12.9% in rGO/Li, aMEGO/Li or AC/Li, respectively), the rGO/Li anode exhibits a low overpotential of ~100 mV for 1500 h, while the aMEGO/Li and AC/Li anodes show an overpotential of ~250 mV under the same measurement conditions. In contrast, the bare Li anode shows fluctuant voltages with a much larger overpotential of > 500 mV (Fig. S8, Supporting Information). When the Li utilization is increased to ~54.9% as in the 100 μm-thick carbon/Li composite anodes, rGO/Li remains stable with a low overpotential of ~200 mV for 1800 h (Fig. 3b). Under the same conditions, the aMEGO/Li anode with a Li utilization of 58.3% behaves like a random oscillation while the AC/Li anode with a Li utilization of 63.5% shows a much larger overpotential (~400 mV) and eventually a short circuit after 500 h. The superior electrochemical performances of rGO/Li can also be supported by the electrochemical impedance spectra. As shown in Fig. 3c and d, the 460 μm rGO/Li ‖ Li cell displays an interface resistance of 0.41 Ω, which is much lower than 5.19, 7.09 and 27.57 Ω for the 460 μm aMEGO/Li ‖ Li, 460 μm AC/Li ‖ Li and 460 μm Li ‖ Li cells, respectively (please see Fig. S9 and Table S3, Supporting Information for the fitting and parameters). The 100 μm rGO/Li symmetrical cell also displays the lowest interface resistance of 70.17 Ω, compared to the 100 μm AC/Li (112.70 Ω) and 100 μm aMEGO/Li symmetrical cells (106.10 Ω) (Table S3, Supporting Information).

To further understand the mechanisms for the different performances of carbon/Li composite anodes, N_2 adsorption-desorption isotherms of rGO, aMEGO and AC were compared. As shown in Fig. 4a, the adsorption and desorption curves of AC are completely overlapped, exhibiting microporous structures. A sharp rise in the adsorption curves of aMEGO and AC observed below $P/P_0 = 0.05$, indicates the existence of a large number of micropores, and the constant rise of the isotherms in the relative pressure range of 0.1–0.4 implies the presence of an appreciable amount of mesopores. The hysteresis loop extending from $P/P_0 = 0.5$ to 0.95 of rGO and from $P/P_0 = 0.4$ to 0.6 of aMEGO, suggests the existence of mesopores [27–29]. Although the specific surface area (SSA) of rGO (~408 m^2/g) is much lower than those of aMEGO (~1850 m^2/g) and of AC (~1264 m^2/g), the pore volume of rGO (~2.366 cm^3/g) is the largest, compared to aMEGO (~1.802 cm^3/g) and AC (~0.757 cm^3/g). It should be also noted that the pores of rGO are dominated by mesopores (size > 4 nm), while aMEGO and AC mainly consist of micropores and mesopores ranging between 1 and 4 nm (Fig. 4b). The size distribution of aMEGO is consistent to previous studies, as the chemical activation is not merely digesting the carbon but also dramatically restructuring the carbon to a porous structure [30]. The morphology of rGO/Li (5Li+6rGO) and aMEGO/Li (5Li+6aMEGO) after the 500th cycle of Li plating performed at 10 mA cm^{-2} for 10 mAh cm^{-2} was investigated and the typical

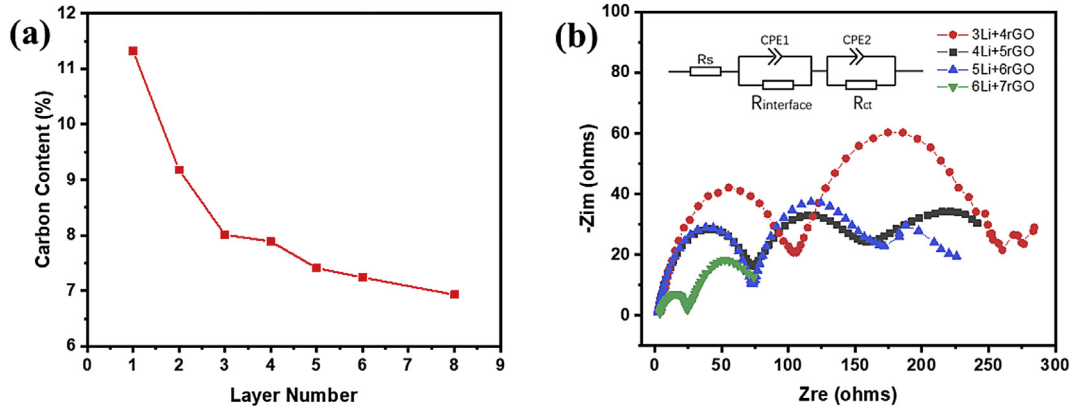

Fig. 2. (a) Relationship between carbon content and layer number for 100 μm rGO/Li composite. (b) Nyquist plots of nLi+(n+1)C symmetrical cells with n of 3, 4, 5, 6, respectively. Inset shows the corresponding equivalent circuit model for fitting.

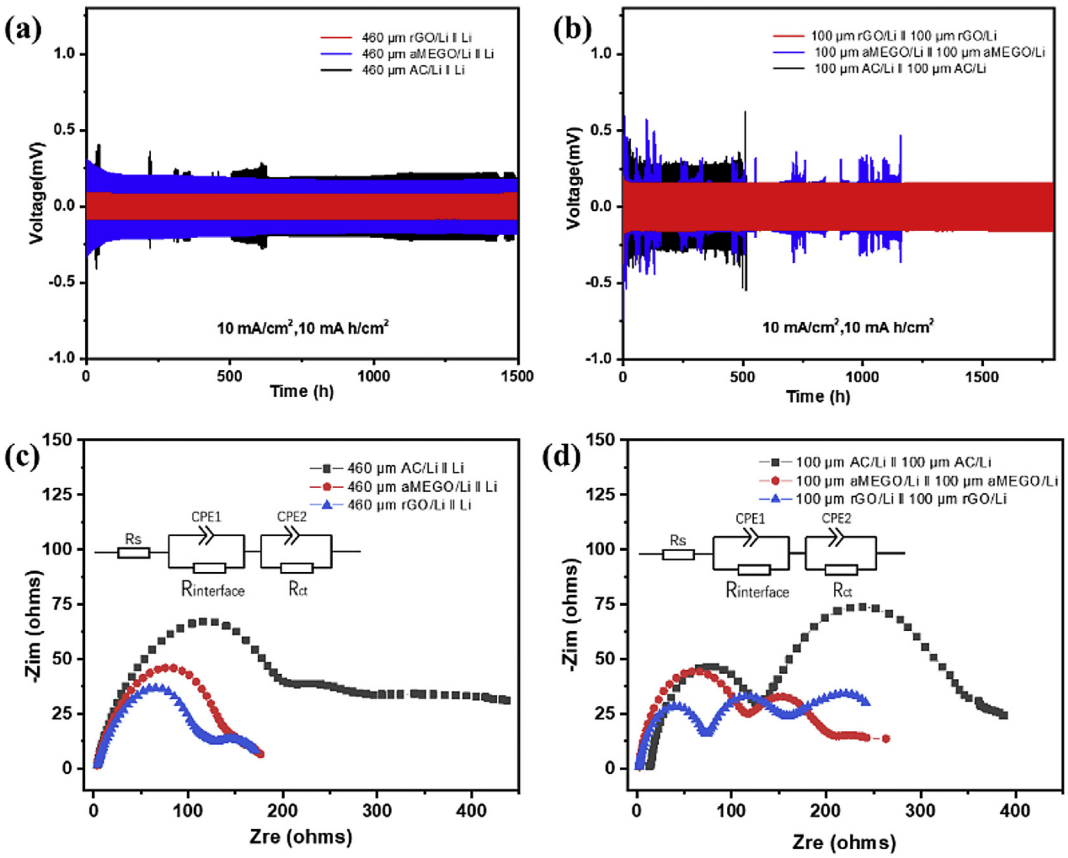

Fig. 3. (a) Cycling performance of carbon/Li composite anodes with a final thickness of 460 μm (obtained from 10Li+11C), measured at a current of 10 mA cm^{-2} for a capacity of 10 mAh cm^{-2}. (b) Cycling performance of carbon/Li composite anodes with a final thickness of 100 μm (obtained from 5Li+6C), measured at a current of 10 mA cm^{-2} for a capacity of 10 mAh cm^{-2}. Nyquist plots of (c) 460 μm carbon/Li ‖ Li cells, (d) 100 μm carbon/Li symmetrical cells. Insets show the corresponding equivalent circuit models.

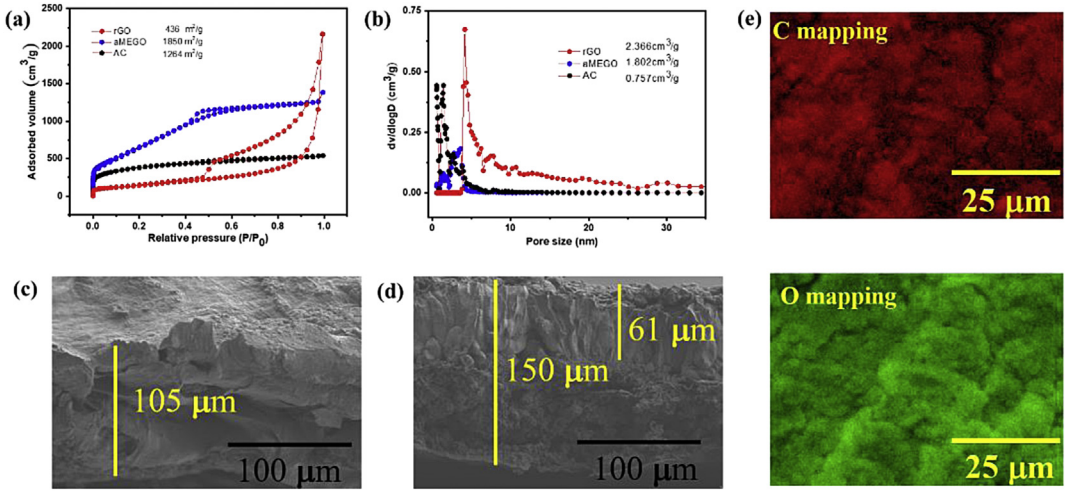

Fig. 4. (a) N_2 adsorption/desorption isotherms of rGO, aMEGO and AC powders. (b) Pore size distribution of rGO, aMEGO and AC powders calculated by density functional theory model. SEM images of (c) 100 μm-thick rGO/Li anode and (d) 100 μm-thick aMEGO/Li anode after the 500th cycle of plating performed at 10 mA cm^{-2} for 10 mAh cm^{-2}. (e) Top view of EDS C and O elemental mapping of rGO/Li after the 500th stripping.

cross-sectional SEM images are shown in Fig. 4c and d. From Fig. 4c we can see that after the 500th plating, the thickness of rGO/Li anode has slightly increased to ~105 μm from original ~100 μm, while the thickness of aMEGO/Li anode significantly increased to ~150 μm (Fig. 4d). As also can be seen from Fig. 4d, cylindric Li with a thickness of ~61 μm is observed on the upper region of the electrode while the lower part seems less compact compared to the upper part. These results suggest that the > 4 nm pores in rGO are able to effectively accommodate Li during repeated plating but the pores in aMEGO may be too small to host Li and thus quite much fraction of Li has been deposited on the surface of aMEGO rather than into the pores. The SEM images in Fig. S10 (Supporting Information) show that AC has pores with a size of ~2 μm, which may also benefit to effectively accommodating Li deposition and explains why AC/Li shows more stable overpotentials than aMEGO/Li for the

situations with the high Li utilization in Fig. 3b [25]. Besides, 'lithiophilic' layered rGO with nanoscaled gaps might also help to stabilize the Li plating by the spacing limitation effect [10]. Fig. 4e and Fig. S11 (Supporting Information) show that, after 500 cycles the carbon distribution remains uniform on Li surface, indicating that the top-coated rGO, AC or aMEGO layer provides an electrochemically and mechanically stable artificial interface that plays a role in stabilizing the as-formed SEI [3,5,10,20]. Generally, rGO acts as both host and artificial interface to stabilize Li, while AC and aMEGO can not efficiently host Li in plating.

Finally, full coin cells have been assembled with $LiNi_{0.5}Co_{0.2}Mn_{0.3}O_2$ (NCM 523) as cathode, and 100 μm rGO/Li (5Li+6C) or 100 μm Li as anodes to demonstrate the feasibility of the composite anodes for applications. As shown in Fig. S12 (Supporting Information), the full cell of 100 μm rGO/Li ‖ NCM 523 retains a specific capacity of 99.6 mA h/g (67.2% of the first cycle) with a Coulombic efficiency of 99.2% after 100 cycles at 0.5C. Under the same conditions, the cell assembled with 100 μm Li foil as the anode delivers a specific capacity of 64.8 mA h/g (44.3% of the first cycle) with a Coulombic efficiency of 96.7% after 100 cycles. Although the full cells need further optimization, the preliminary comparison confirms that the rGO/Li (5Li+6rGO) electrode performs better than the bare Li with the same thickness when being used with NCM 523 in terms of capacity retention and rate capacity.

4. Conclusion

In summary, we have fabricated carbon-modified Li metal anodes by rolling press, which can be considered as a facile and effective way to prestore Li for scalable production. The composite anodes demonstrate high areal capacity of 10 mAh cm^{-2} cyclable at high current density of 10 mA cm^{-2} for 1500 h. Among the carbons investigated, the rGO/Li anode shows the lower overpotentials and the more stable cycling performance than the other two. The superior electrochemical performance of rGO/Li anode is attributed to the high pore volume and moderate pores size of rGO, which could accommodate the volume change. The rational design of Li-metal anodes by rolling press may promote the realization of scalable production of high-performance Li metal batteries.

Data availability

The raw/processed data required to reproduce these findings cannot be shared at this time as the data also forms part of an ongoing study.

Acknowledgements

This work was supported by the Natural Science Foundation of China (51772282) and funding from Hefei Center for Physical Science and Technology.

Appendix A. Supplementary data

Supplementary data to this article can be found online at https://doi.org/10.1016/j.ensm.2019.07.044.

References

[1] W. Xu, et al., Lithium metal anodes for rechargeable batteries, Energy Environ. Sci. 7 (2) (2014) 513–537.
[2] D. Lin, Y. Liu, Y. Cui, Reviving the lithium metal anode for high-energy batteries, Nat. Nanotechnol. 12 (3) (2017) 194.
[3] K. Yan, et al., Ultrathin two-dimensional atomic crystals as stable interfacial layer for improvement of lithium metal anode, Nano Lett. 14 (10) (2014) 6016–6022.
[4] T. Foroozan, et al., Synergistic effect of graphene oxide for impeding the dendritic plating of Li, Adv. Funct. Mater. 28 (15) (2018) 1705917.
[5] M. Bai, et al., A scalable approach to dendrite-free lithium anodes via spontaneous reduction of spray-coated graphene oxide layers, Adv. Mater. (2018) 1801213.
[6] Y. Zhao, et al., Carbon paper interlayers: a universal and effective approach for highly stable Li metal anodes, Nano Energy 43 (2018) 368–375.
[7] D. Zhang, et al., The effect of the carbon nanotube buffer layer on the performance of a Li metal battery, Nanoscale 8 (21) (2016) 11161–11167.
[8] J. Qian, et al., High rate and stable cycling of lithium metal anode, Nat. Commun. 6 (2015) 6362.
[9] W. Li, et al., The synergetic effect of lithium polysulfide and lithium nitrate to prevent lithium dendrite growth, Nat. Commun. 6 (2015) 7436.
[10] D. Lin, et al., Layered reduced graphene oxide with nanoscale interlayer gaps as a stable host for lithium metal anodes, Nat. Nanotechnol. 11 (7) (2016) 626.
[11] W. Deng, et al., Microscale lithium metal stored inside cellular graphene scaffold toward advanced metallic lithium anodes, Adv. Energy Mater. (2018) 1703152.
[12] S. Liu, et al., Crumpled graphene balls stabilized dendrite-free lithium metal anodes, Joule 2 (1) (2018) 184–193.
[13] L. Liu, et al., Uniform lithium nucleation/growth induced by lightweight nitrogen-doped graphitic carbon foams for high-performance lithium metal anodes, Adv. Mater. 30 (10) (2018) 1706216.
[14] J. Xie, et al., Incorporating flexibility into stiffness: self-grown carbon nanotubes in melamine sponges enable a lithium-metal-anode capacity of 15 mA h cm− 2 cyclable at 15 mA cm− 2, Adv. Mater. (2018) 1805654.
[15] S. Jin, et al., High areal capacity and lithium utilization in anodes made of covalently connected graphite microtubes, Adv. Mater. 29 (38) (2017).
[16] Z. Sun, et al., Robust expandable carbon nanotube scaffold for ultrahigh-capacity lithium-metal anodes, Adv. Mater. (2018), e1800884.
[17] Y. Liu, et al., Lithium-coated polymeric matrix as a minimum volume-change and dendrite-free lithium metal anode, Nat. Commun. 7 (2016) 10992.
[18] Z. Liang, et al., Composite lithium metal anode by melt infusion of lithium into a 3D conducting scaffold with lithiophilic coating, Proc. Natl. Acad. Sci. 113 (11) (2016) 2862–2867.
[19] R. Zhang, et al., Coralloid carbon fiber-based composite lithium anode for robust lithium metal batteries, Joule 2 (4) (2018) 764–777.
[20] B. Li, et al., Flexible Ti3C2 MXene-lithium film with lamellar structure for ultrastable metallic lithium anodes, Nano Energy 39 (2017) 654–661.
[21] M.S. Kim, et al., Langmuir–Blodgett artificial solid-electrolyte interphases for practical lithium metal batteries, Nat. Energy 3 (10) (2018) 889.
[22] X. Shen, et al., Lithium–matrix composite anode protected by a solid electrolyte layer for stable lithium metal batteries, J. Energy Chem. 37 (2019) 29–34.
[23] H. Ye, et al., Advanced porous carbon materials for high-efficient lithium metal anodes, Adv. Energy Mater. 7 (23) (2017) 1700530.
[24] W. Liu, et al., Stabilizing lithium metal anodes by uniform Li-ion flux distribution in nanochannel confinement, J. Am. Chem. Soc. 138 (47) (2016) 15443–15450.
[25] C.-P. Yang, et al., Accommodating lithium into 3D current collectors with a submicron skeleton towards long-life lithium metal anodes, Nat. Commun. 6 (2015) 8058.
[26] J. Xie, et al., Incorporating flexibility into stiffness: self-grown carbon nanotubes in melamine sponges enable a lithium-metal-anode capacity of 15 mA h cm^{-2} cyclable at 15 mA cm^{-2}, Adv. Mater. 31 (7) (2019) 1805654.
[27] L. Xie, et al., Hierarchical porous carbon microtubes derived from willow catkins for supercapacitor applications, J. Mater. Chem. 4 (5) (2016) 1637–1646.
[28] Q. Liang, et al., A honeycomb-like porous carbon derived from pomelo peel for use in high-performance supercapacitors, Nanoscale 6 (22) (2014) 13831–13837.
[29] X. Zhu, et al., Porous three-dimensional activated microwave exfoliated graphite oxide as an anode material for lithium ion batteries, RSC Adv. 6 (60) (2016) 55176–55181.
[30] Y. Zhu, et al., Carbon-based supercapacitors produced by activation of graphene, Science 332 (6037) (2011) 1537–1541.